ORIGINAL

Mixed numerical–experimental methods in wood micromechanics

**E. Kristofer Gamstedt · Thomas K. Bader ·
Karin de Borst**

Abstract   Mixed numerical–experimental methods are increasingly used in various disciplines in materials science, recently also in wood micromechanics. Having a relatively irregular microstructure, direct interpretation of mechanical tests is not always possible since structurally specific properties are quantified rather than general material properties. The advent of combined numerical–experimental methods unlocks possibilities for a more accurate experimental characterization. A number of examples of mixed methods pertaining to both emerging experimental techniques and physical phenomena are presented: nano-indentation, moisture transport, digital-image correlation, dimensional instability and fracture of wood-based materials. Successful examples from other classes of materials are also presented, in an attempt to provide some ideas potentially useful in wood mechanics. Some general pit-falls in parameter estimation from experimental results are also outlined.

Introduction

The use of mixed numerical–experimental techniques is gaining increased use in materials science. With the combination of numerical models, significantly more

E. K. Gamstedt (✉)
Department of Engineering Sciences, Applied Mechanics, Uppsala University,
Box 543, SE-751 21 Uppsala, Sweden
e-mail: kristofer.gamstedt@angstrom.uu.se

T. K. Bader
Institute for Mechanics of Materials and Structures, Vienna University of Technology,
Karlsplatz 13/202, 1040 Vienna, Austria

K. de Borst
School of Engineering, University of Glasgow, Rankine Building (R703), Glasgow G12 8LT,
Scotland, UK

information could be gained from experiments. In principle, measured physical values, for example, displacements, strains, loads or velocities, are compared with corresponding results in a numerical model, such that physical measurements and predicted results match by tuning model parameters. Such an approach has led to new opportunities in the design of experiments for characterization of material properties, otherwise intractable to quantification. Mixed numerical–experimental methodologies can also be regarded as a discipline in itself, where the development of procedures for robust identification of material parameters is the main goal (Tarantola 2005), although it is in the applications where the mixed methods are of best service. A schematic illustration of a methodology to identify material properties not readily available by direct measurements is found in Fig. 1. The mixed numerical–experimental methods have mostly been used for high-performance structural materials, like carbon-fibre composite laminates, which like wood are anisotropic and microscopically heterogeneous. The use of mixed methods for wood materials is still gaining momentum and has not reached its full potential. For composites, for example, conference books (Sol and Oomens 1997; Waszczyszyn et al. 2009), book chapters (Rikards 2003) and review papers (Vantomme et al. 1995; Bonnet and Constantinescu 2005) on mixed numerical–experimental methods have been compiled, whereas for wood materials, only a recent workshop within COST Action FP0802 specifically targeted towards mixed methods has been identified (Morais et al. 2011). The successful use of mixed approaches for other materials can be used as an inspiration for applications in wood material science.

A common paradox in experimental mechanics to characterize mechanical properties is that it could be experimentally very difficult to obtain a direct measurement of a sought mechanical property, and advanced inverse modelling may be required to identify the property from a simple and more direct experiment. A classic example is the elastic tensile modulus of wood along the grain, which should ideally be characterized by tensile testing with a uniform tensile stress in the grain direction. This is, however, not easy since the soft cellular microstructure often leads to transverse crushing when the sufficient clamping forces are applied to reach the necessary tensile loads in the longitudinal direction (e.g. Bonfield and Ansell 1991). Slippage and premature breakage can then obstruct the measurement of the elastic tensile modulus. Three point bending is, however, straightforward to perform, although the elastic tensile modulus cannot be directly identified since
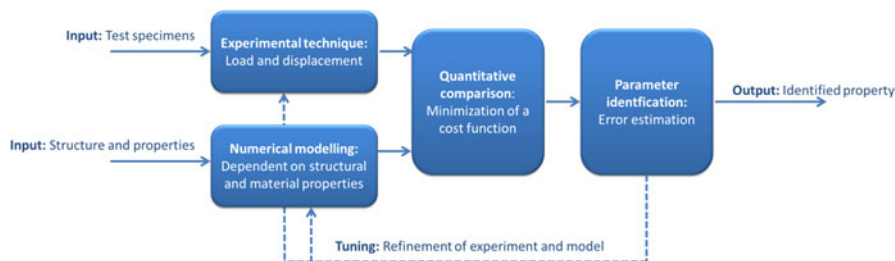

Fig. 1 Schematic of mixed experimental–numerical approach to identify properties not readily quantified by direct measurements alone

shear stresses are present (e.g. Yoshihara and Tsunematsu 2007), especially for specimens that are not exceedingly slender. Other complicating factors are that the elastic tensile and compression moduli may differ for materials with a wood-like cellular structure (Gibson et al. 1981) and that the low shear modulus can contribute significantly to the elastically polar orthotropic wooden beams (Shipsha and Berglund 2007). Instead, an effective stiffness value, that is, the modulus of elasticity (MOE), pertinent to the specific bending test method is commonly used. However, the elastic tensile modulus would generally be preferred to the MOE, since it is a material property, ideally independent of test method and specimen geometry. Still, the simplicity of a straightforward experimental method can be advocated, if combined with an adequate numerical model that accounts for the geometry of the test body and the necessary details of the inherent material microstructure and anisotropy. Material properties could thus be obtained from simple tests, in a general sense, as will be illustrated with a variety of examples in the subsequent sections. To achieve this, a necessary complement to the experiments is computational mechanics. The field of computational mechanics has evolved from engineering design of structures and entered materials science. An increasing part of research in computational mechanics is devoted to cross-disciplinary interaction with experimental materials science. A promising area of research is to integrate computational and experimental mechanics further to develop improved mixed numerical–experimental methods, applicable in, for example, quantitative materials design and identification of elusive material properties.

The purpose of this paper is to review some successful efforts using mixed numerical–experimental methods in wood micromechanics, which can hopefully inspire some new ideas in this research area. The unique microstructure of wood is taken into consideration in most of the subsequent examples. The following topics will briefly be addressed: microscale deformation from digital-image correlation, local elasticity from nano-indentation, fracture mechanics, moisture transport and dimensional instability. Also, a couple of 'success stories' of mixed numerical–experimental methods applied to other materials are presented, which could in principle also be adopted for wood materials. A number of pitfalls are identified, followed by an outlook with future prospects.

Examples

Microscale deformations from digital-image correlation

The increasing trend to unravel the origin of the macroscopic behaviour of materials at smaller length scales has motivated efforts for developing digital-image correlation (DIC) systems also for microscale applications. A successful strategy has been presented by Schreier et al. (2004), who combined the standard camera imaging system with a stereo microscope. The main challenges in this context concern the removal of the complex image distortions, which might result from the combination of possible aberrations of lens, mirror, and prism with an imperfect alignment of lenses.

The application of this micro-DIC system for investigating deformations of a common mouse carotid artery vessel subjected to internal pressure is shown by Sutton et al. (2008). Quasi-static as well as cyclic test conditions were investigated. Typical dimensions of such an artery vessel are 0.4 mm in diameter and 5–8 mm in length. A speckle pattern was applied to the exterior of the carotid specimen on the basis of a contrast enhancer (toner powder coating the specimen). All tests were performed with a 2.5× magnification and a field of view sized 2 mm by 2 mm. Typically, displacements down to 1/100th of the dimensions of the field of view can be resolved. Based on the measured displacements, average longitudinal and transverse strains of the vessel were determined over a data analysis area sized 50 μm × 250 μm (cf. Fig. 2), and the onset of nonlinear constitutive behaviour was studied. Moreover, inhomogeneities in the displacement maps were studied in order to identify microstructural variations relevant for the mechanical response. Finally, in-plane elastic moduli of the tissue were derived from the measured average strains, after fixing the Poisson ratios to realistic values.

The wall of blood vessels exhibits a similar multi-layered, fibre-reinforced microstructure to wood cell walls. The suitability of a DIC system for assessing out-of-plane deformations and the twist of a specimen renders it attractive for accompanying single fibre tests. Similar to the strategy described in Sutton et al. (2008), the DIC system could be used to assess variations of the fibre behaviour, resulting from structural or material changes, along the measurement length. However, the stiffness of the carotids investigated by the group around Sutton is by a factor of more than 100 smaller than that of wood cells. This results in considerably smaller deformations and, consequently, higher requirements on

Fig. 2 Schematic sketch of measurement system and example image of a pressurized artery vessel obtained with the cameras
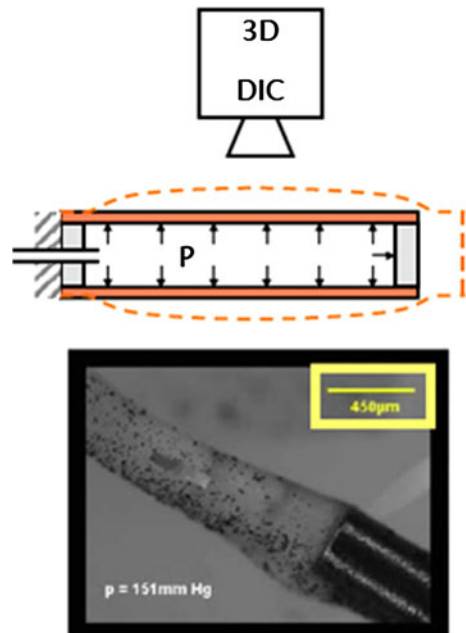
resolution for measuring strains in wood cell walls. This might constitute a future challenge for further development of microscale DIC systems.

An informative review of various mixed methods to obtain elastic properties from full-field deformation measurements such as DIC of complex bodies has been compiled by Avril et al. (2008). A number of numerical methods are compared in combination with a couple of mechanical test methods, and advantages and drawbacks of the various combinations are discussed. In particular, the sensitivity to noise in input data was apparent. Although computationally more costly, numerical methods based on updating procedures are recommended to reduce the noise sensitivity. In these methods, displacement fields are computed by finite element simulations using initial guesses for the elastic parameters. The actual parameters are identified by minimizing a least-square distance function where the available measurements are compared to their computed counterparts for each deformation step.

Local elasticity determined from nano-indentation

One aim of indentation techniques is to measure elastic properties of a material at micrometre scale. This is done by pressing an indenter with a predefined geometry under load control into a material, while the indentation depth is continuously measured. Hardness is then derived as the maximum applied force over the projected area of contact. From the unloading part of the load–indentation depth relationship, additionally, an elastic modulus can be obtained, usually termed indentation modulus or reduced modulus M since the indenter compliance is taken into account (Oliver and Pharr 1992). However, this quantity is not directly comparable to elastic properties of the tested material. For isotropic materials, M is independent of the indentation direction and depends on two elastic constants (Pharr et al. 1992). In general, however, this elastic quantity is influenced by the anisotropy of the tested material and the indentation direction. Hence, for identification of material parameters from indentation moduli of anisotropic materials, a mechanical model is required (Swadener and Pharr 2001; Vlassak et al. 2003).

As described in more detail in Eder et al. (2012), nano-indentation can be applied for measuring mechanical properties of the cell wall of wood fibres. Particularly, the S_2 layer as the thickest and mechanically dominant layer has been tested (Fig. 3). The highly aligned orientation of the cellulose fibrils in this layer results in anisotropic elastic properties. The mechanical behaviour in microfibril direction can be approximated as transversely isotropic (Jäger et al. 2011b). Consequently, the indentation modulus M depends on five elastic constants of the cell wall material (elastic moduli E_L, E_T, G_{TL} and Poisson's ratios v_{TT}, v_{TL}) and the indentation direction relative to the cellulose fibrils orientation δ, reading as

$$M = f\left(E_L, E_T, G_{TL}, v_{TT}, v_{TL}, \delta\right).$$

In case of indentation in fibre direction, δ can be substituted by the microfibril angle (MFA). Anisotropic indentation theory was recently applied to wood by Jäger et al. (2011a). Their work is based on the theoretical problem of indentation of a rigid frictionless conical indenter into an elastically anisotropic half space presented

Fig. 3 a Cellular structure of softwood (*Picea abies* L.) with earlywood (EW) and latewood (LW) tracheids. **b** Detail of cell wall of latewood tracheid, showing the secondary 2 *layer* (S$_2$) with imprints of NI tests and the cell corner middle lamella (CML). **c** Indentation of a cone into an elastically anisotropic half space (Jäger et al. 2011a)

by Vlassak et al. (2003). Parameter studies revealed that the indentation modulus of the S$_2$ layer of wood fibres mainly depends on the elastic moduli E_L, E_T, G_{TL}, while the influence of Poisson's ratios is negligible. Moreover, a nonlinear relationship between M and MFA was presented (Jäger et al. 2011a). In order to quantify the elastic constants of the S$_2$ cell wall material from indentation tests, testing in at least five different indentation angles in relation to the orientation of the microfibrils is required. For one latewood band of spruce (*Picea abies*), the whole range of possible indentation angles from 0° to 90° was investigated by Jäger et al. (2011b), see Table 1.

   In order to identify elastic constants from these test data, the nano-indentation model is employed, which gives the relation between M and the indentation direction for a specific set of elastic constants. An error minimization procedure yields the sought elastic parameters of the cell wall material. Because of their small influence, the Poisson ratios cannot be determined in this reverse identification. They are estimated as v_{TT}, $v_{TL} = 0.3$ in the given example. This yields the other elastic moduli as $E_T = 4.54$ GPa, $E_L = 26.32$ GPa and $G_{LT} = 4.84$ GPa in relation to the principal material directions of the cell wall.

Table 1 Measured indentation moduli M (mean values) at specified inclination angles δ between indentation direction and microfibril orientation (reproduced from Jäger et al. (2011b); only one indent in tangential cell wall of sample 5)

Sample	1		2		3		4		5	
Radial cell walls										
δ [°]	8.59	10.12	1.01	16.43	24.12	41.26	37.24	54.44	72.10	89.32
M [GPa]	16.37	16.86	19.20	17.36	14.32	11.50	11.40	8.86	6.35	6.02

Sample	1		2		3		4		5
Tangential cell walls									
δ [°]	4.98	12.34	11.10	12.01	32.92	33.86	46.38	46.59	80.71
M [GPa]	16.03	15.84	16.19	14.94	9.49	11.32	8.12	9.28	5.89

The mean error between reduced moduli predicted with these elastic constants and the measured moduli amounts to only 8 %. This underlines the suitability of the model and, in particular, the assumption of transversely isotropic mechanical behaviour of the cell wall material. A prerequisite for an accurate and robust parameter identification is the availability of test data over the whole range of indentation angles (Konnerth et al. 2010; Jäger et al. 2011b).

In order to further verify the mixed numerical–experimental approach, data for the cell wall stiffness obtained from other methods are invoked. Tension tests on small-sized samples and single fibres as well as micro-bending tests on cell wall segments are considered (Jäger et al. 2011b). Since all these methods assess the entire cell wall, the resulting elastic moduli are expected to fall below those derived on basis of the nano-indentation tests, probing exclusively of the (stiffest) S_2 layer. The results are summarized in Table 2.

Table 2 Elastic moduli of the cell wall measured with different experimental techniques, reproduced from Jäger et al. (2011b) and extended with results from Eder et al. (2012)

Method	MFA [°]	E_L [GPa]	E_T [GPa]	Comment	Reference
Tension small-sized samples (2 × 2 mm^2)	0	41		Radiata pine; fifth internode; 10 % RH	Cave (1969)
	5	14		Norway spruce; wet conditions	Reiterer et al. (1999)
	12		0.7–4.5	Swedish Norway spruce; EW, TW and LW across one annual ring wet conditions	Bergander and Salmén (2000a, b)
Tension single fibres	7–13.6	16.1–26		Austrian Norway spruce; EW and LW from pith to bark; wet conditions	Eder et al. (2009)
	0–5	26.2		Norway spruce; adult heartwood; 65 % RH	Keunecke and Niemz (2008)
	5–17.5	13.9–26.2		Common yew and Norway spruce; adult TW; 65 % RH	Keunecke et al. (2008)
		22.6		Norway spruce; adult TW	Burgert et al. (2003)
		15–23		Norway spruce, adult late TW; 65 % RH	Burgert et al. (2005)
	5.8–43.6	5.1–27.5		Southern pine, EW and LW (incl. juvenile wood), dry conditions, chem. isolated	Mott et al. (2002)
	15.2–34.9	9–20		Chinese fir, LW (juvenile and mature); 40 % RH; chem. isolated	Wang et al. (2011)
Micro-bending		28		Norway spruce; vacuum dry	Orso et al. (2006)

EW earlywood, *LW* latewood, *TW* transition wood

The elastic moduli obtained with the mixed approach refer to moduli at zero MFA. When comparing them with the data for single fibres in Table 2, it also has to be taken into account that fibres generally can twist to a certain extent (Neagu et al. 2006), while complete rotational restraint is assumed in the model of the mixed approach. This will result in higher moduli obtained in the mixed approach compared with the fibre moduli. As regards the results of the micro-bending tests on cell wall specimens (Orso et al. 2006), the influence of testing the entire cell wall and not only the S_2 layer takes largest effect here. Due to the bending deformation, the outermost (weaker) cell wall layers contribute over-proportionally to the measured stiffness.

On the whole, the longitudinal modulus obtained with the mixed approach seems to be rather low. This could be a consequence of possible buckling or kinking of microfibrils in compression (in the plastically affected volume under the indenter) or bending under transverse loading, which all are not taken into account in the model. An extension of the anisotropic indentation model to a fibrous (inhomogeneous) material might help to further improve the model performance.

The combined numerical–experimental approach allows bringing the information obtained from nano-indentation tests from a merely qualitative level in most current applications to a quantitative level. The wide range of applications of nano-indentation in wood science, particularly in relation to wood modification as outlined in Eder et al. (2012), will profit from this development.

Fracture mechanics

Being a polymer material, wood shows outstanding fracture resistance. The tree trunk should carry significant load from the weight of the tree itself and from bending caused by storms. The hierarchical structure of wood (Fratzl and Weinkamer 2007) means that fracture planes and preceding zones of inelastic deformation can occur on several structural length scales. The near-fractal appearance of wood fracture perpendicular to the grain direction shows a multiscale fracture process, with dissipation mechanisms on several length scales. This results in an impressively high fracture toughness compared with other polymer materials. Even in the weakest plane, that is, along the grain direction, wood is a tough material, which can readily be confirmed by anyone who has tried to chop knot-rich wood with an axe. Direct observation of crack growth in mode I wedge loading of wood shows crossover fibre bridging in the wake of the crack tip, as schematically depicted in Fig. 4a. This mechanism results in a large-scale bridging zone which contributes significantly to the fracture toughness. The mechanism of crossover fibre bridging has been observed in intralaminar cracking of unidirectional fibre composites (Spearing and Evans 1992), also shown in Fig. 4b. The cohesive zone model or bridging law, expressed as cohesive traction as a function of crack opening displacement, can be regarded as a material property which has significant impact on fracture toughness in materials where large-scale bridging zones tend to develop, such as in splitting of wood along the grain. Given the cohesive law, the geometry-dependent R-curve, that is, the energy release rate vs. crack length, can be estimated using a J-integral approach (Sørensen and Jacobsen 1998),
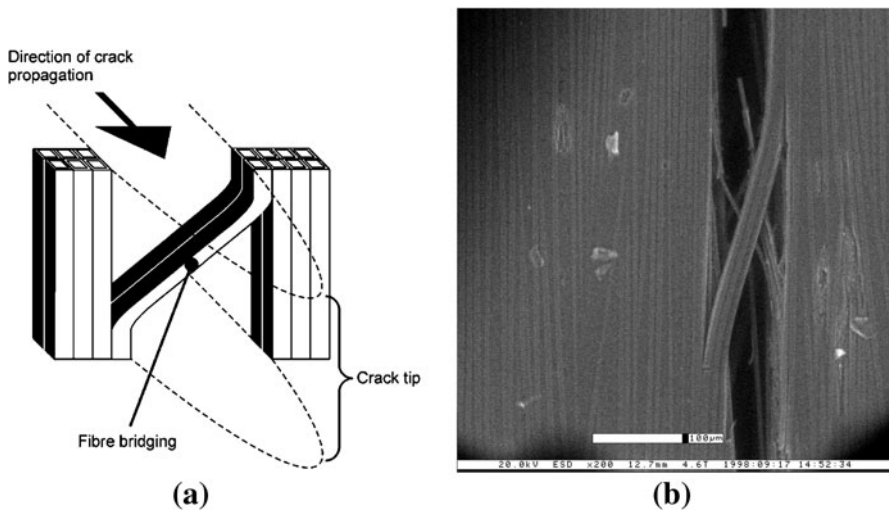
Fig. 4 a Schematic illustration of observed fibre bridging in fracture of wood (Keunecke et al. 2007) and **b** scanning-electron micrograph of crossover fibre bridging in intralaminar cracking a unidirectional carbon-fibre reinforced composite (Sørensen et al. 2008)

$$J(a) = \int_{0}^{\delta*} \sigma(\delta)\, d\delta + J_{tip}$$

where $J(a)$ is the J-integral for a crack of length a, σ is the cohesive traction, δ is the crack opening displacement, δ^* is the end-opening displacement and J_{tip} is the energy dissipated at the crack tip in front of the cohesive zone. However, the cohesive law is not readily determined from tensile loading of double-cantilever beam specimens loaded in tension, since $J(a)$ cannot be found directly from easily measured loads and displacements (Sørensen and Jacobsen 2003). A mixed numerical–experimental method is a way forward, which combines a relatively simple mechanical tensile test and a model that produces a cohesive material property, which can be used to predict fracture toughness for arbitrary load conditions and geometries.

Since wood tends to show large-scale damage zone on fracture, linear elastic fracture toughness is generally not directly applicable. The next step of generalization is to formulate and characterize the cohesive law, with which fracture processes could be predicted more accurately. In the quest to characterize the cohesive law, the relative efforts in complementary modelling and experimental work can be considered. One may consider a more complex experimental set-up, for example, with pure bending moments in a double-cantilever beam test and a more direct model, where the cohesive law is determined through the derivate of the J-integral which is estimated directly from the moments (Sørensen and Jacobsen 2003). On the other hand, if laboratory set-up is limited to simple tensile testing of the double-cantilever beam, a more complicated numerical model involving integral

equations with weight function contributions from the cohesive zone to the stress intensity factor can be adopted to still quantify the cohesive law (Östlund and Nilsson 1993). Essentially, the relative complexity or simplicity of matching the experimental and the numerical method should be considered before starting to develop new mixed methods. The balance in this trade-off is of course dependent on the experience and the experimental facilities at hand in the laboratory that undertakes the task to develop mixed method.

Moisture transport

Moisture ingress is generally considered to be a nuisance in wood materials. It leads to softening, degradation of mechanical properties and susceptibility to microbial attack. The physical basis of the interactions between wood and water is discussed in Engelund et al. (2012) in detail. A better understanding of how moisture is transported into the wood materials would provide useful knowledge how to prevent moisture uptake. Being a rather complex mechanism dependent on microstructure and external conditions, a mixed numerical–experimental approach can prove useful in addressing these transport phenomena.

As outlined in Engelund et al. (2012), moisture transport in wood below the fibre-saturation point involves several processes: diffusion of water vapour in the cell pores, diffusion of bound water in the cell walls, and sorption at the cell wall surfaces. In order to suitably describe the behaviour of wood during changes of the moisture content, such as drying or wetting, all three processes have to be considered individually (Perré 2007; Krabbenhoft and Damkilde 2004; Eitelberger et al. 2011b). If only a single Fickian equation is used at the macroscopic scale in a simplified manner, the so-called non-Fickian effects are encountered like dependency of the diffusion coefficients on the sample thickness (Absetz 1999). Convective boundary conditions have also shown to account for non-Fickean diffusion (Olek et al. 2011). Furthermore, it has turned out that also the heat transformations upon sorption recognisably affect the transport behaviour, which have been included in an extended model by Eitelberger et al. (2011b).

The above-mentioned processes are mainly governed by the diffusion coefficients of water vapour in the pore structure and of bound water in the cell wall material as well as by the sorption rate. These properties cannot be determined from a conventional sorption test, in which the mass increase in a wood sample is measured during changing environmental humidity. The effects of the different processes appear in a superimposed manner. Moreover, the diffusion and sorption properties depend on moisture content and temperature, which prevents their direct identification from tests involving inhomogeneous moisture distributions occurring during drying and wetting.

In order to resolve non-homogeneous, time-dependent distributions of water in wood, nuclear magnetic resonance (NMR) imaging (also termed magnetic resonance imaging, MRI) was introduced to wood science (e.g. Quick et al. 1990; MacMillan et al. 2002; Hameury and Sterley 2006; Dvinskikh et al. 2011).

The NMR signal is proportional to the local total moisture content but still does not allow separating different phases and transport phenomena. This can be

achieved by combining experimental investigations with numerical simulations, in which the unknown microstructural material properties are tuned such that the predicted system response agrees with the measured one. Such strategies are already well established for other porous building materials (e.g. Pel et al. 1996 for drying of brick and gypsum, Nguyen et al. 2008 for coupled ion and moisture transport in plaster and sandstone).

Recently, a combined numerical–experimental investigation of moisture transport employing NMR imaging was also carried out for wood by one of the authors. Therein, moisture profiles in cylindrical wood samples with diameters of approximately 7.9 mm were measured in the three principal material directions (longitudinal, radial, tangential) at step changes of relative humidity (65 % → 95 % RH, 95 % → 35 % RH, 35 % → 65 % RH) (Dvinskikh et al. 2011; Eitelberger et al. 2011a). For that purpose, the samples were sealed on all sides except for one, which was exposed to air with a controlled relative humidity adjusted by different salt solutions, and placed into an NMR tube (see Fig. 5 for the test setup). Constant time imaging was used and NMR settings of phase encoding time 70 μm and rf pulse length 0.5 μm (Eitelberger et al. 2011b). The investigated area had a length of 16 mm, extending from the sample surface inwards.

Moisture profiles were measured at increasingly distant time instants until equilibrium conditions were reached in the sample. In an exemplary manner, the profile in radial direction is shown in Fig. 6 for the first humidity step (65 % → 95 % RH) exhibiting absolute moisture contents between 25 and 125 kg/m^3. The mass of water is always related to the volume in the dry state as common reference. The peaks in the moisture content are related to the latewood bands, in which the higher fraction of cell wall allows to adsorb more water compared with the earlywood sections with larger lumens. With increasing time of exposure of the sample, more and more water is adsorbed resulting in a shift of the moisture profiles to higher moisture contents. In order to relate the measured absolute amount of water in the sample to the mass density and, thus, to derive the local moisture content u, the samples had been analysed by Silviscan (Evans 1999, 2006) to obtain the corresponding density profiles.

Besides the experimental efforts, a numerical model was established for studying transient, non-homogeneous moisture distributions in wood during drying or wetting events (Eitelberger et al. 2011a). The macroscopic formulation of this

Fig. 5 Experimental setup in NMR device for measuring moisture profiles
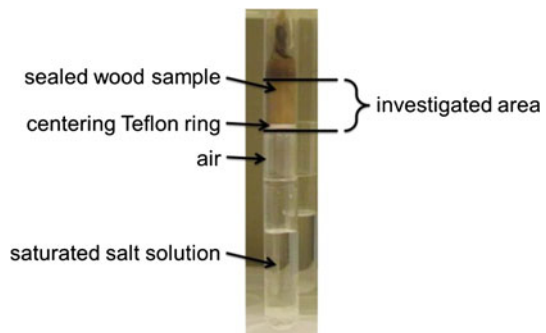
model is based on three coupled differential equations, describing the conservation of mass of bound water, of mass of water vapour, and of heat. Weak couplings in terms of the dependence of the moisture transport properties on temperature and of the heat conduction properties on the moisture content as well as strong couplings in terms of sorption and associated heat changes are considered therein. The sorption rate is determined from a microscale sub-model, in which the moisture transport in a single cell wall and the corresponding moisture transfer at the surface are resolved. The material properties in the macroscopic formulation are estimated by means of multiscale models from the microstructure of wood and material properties at smaller length scales (Eitelberger and Hofstetter 2010a, b). Finally, the system of differential equations is solved numerically in the framework of a finite element code (Eitelberger et al. 2011a).

   Diffusion characteristics of the cell wall play a central role in both the multiscale model and the sorption sub-model. Applying a combined mixed-experimental strategy, the bound water diffusivities of the cell wall in longitudinal and transverse direction, $D_{cw,L/Trans}$, can be back-calculated from the macroscopic model response observed in the experiments (cf. Fig. 6). The functional relation to be solved by the model is

$$D_{cw,L/Trans} = f\left(D_{wood,L/R/T}, D_{vapour}, \text{ cell structural parameters}\right),$$

where $D_{wood,L/R/T}$ denotes the macroscopic (apparent) diffusion coefficients in L/R/T-direction, and D_{vapour} the vapour diffusivity of moist air. The cell structural parameters were obtained from the Silviscan investigations. D_{vapour} was derived from a semi-empirical, temperature-dependent relation following Schirmer (1938) as described in Eitelberger et al. (2011b) in detail, taking additionally into account the different hindrance of the vapour flow by the cell wall structure in the different anatomical directions of wood (see also Engelund et al. 2012).

   Using $D_{cw,L} = 2.5\,D_{cw,trans}$ (Siau 1984), values of $D_{cw,trans} = 3.43 \times 10^{-12}$ m²/s and $D_{cw,L} = 8.57 \times 10^{-12}$ m²/s are obtained at a temperature of 26.7 °C (corresponding to 300 K) and a moisture content of 0.1. The good agreement of
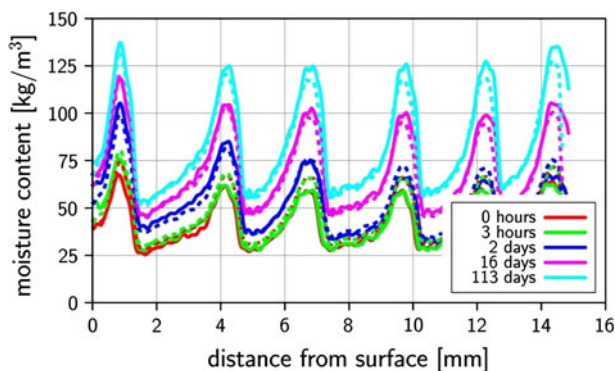

Fig. 6 Moisture profiles in radial direction at different time instants: comparison of test results (*solid lines*) and corresponding model predictions (*dashed lines*)

the profiles predicted by the model using these values (dashed lines in Fig. 6) with the corresponding experimental results underlines the suitability of both the model for moisture transport and its use for reverse identification of material parameters at the cell wall scale. Engelund et al. (2012) refer to permeability measurements on thin films of wooden polymers in order to estimate the bound water diffusion coefficient of wood. They specify a range of $0.1–7 \times 10^{-12}$ m²/s for tests on cellophane films and arabinoxylan films. At a temperature of 26.7 °C (corresponding to 300 K) and a moisture content of 0.1, the analytical relation proposed herein yields $D_{\text{cw,trans}} = 3.43 \times 10^{-12}$ m²/s and $D_{\text{cw,L}} = 8.57 \times 10^{-12}$ m²/s, which are values in a similar range.

In order to further verify the back-calculated diffusivity, the formulation for $D_{\text{cw,L/trans}}$ is used in applications of the moisture transport model other than the re-simulated NMR tests, for which corresponding test data exist. As an example, cup tests on thin wood specimens (1.55–6.25 mm thickness in L-direction) are considered (Eitelberger and Svensson 2012). The increase in the moisture content of the sample in a controlled change of the environmental humidity could be well reproduced by the model (Eitelberger and Hofstetter 2011). This confirms the suitability of the determined diffusion characteristics. Certainly, one has to keep in mind that the model used for the reverse identification is employed here also for the prediction. However, the greater the number and variety of physical observations a model can describe, the higher the certainty that its formulation and its parameter are suitable. In the presented applications, numerical simulations were mainly applied to bridge length scales and to resolve inhomogeneities in the investigated samples. Intrinsic material properties of microscale components, such as cell wall substance in wood, can be linked to experimentally accessible, macroscopic properties, such as the apparent moisture diffusivity. In a next step, such a bridge could also be established between time scales. Such attempts have been made for clay colloids in the framework of studies on the long-term mobility of diffusing probes (Porion and Delville 2009). A multiscale model based on a sequence of quantum mechanical and molecular dynamical steps was used to fill the gap between the time scales that can be studied in NMR tests (typically a few ms up to 1 s) and the molecular mobility of interest (<1 ns). Fields of application of these studies are optimization tasks in industrial processes like waste storing and heterogeneous catalysis, in which the physico-chemical properties of clay colloids are exploited. Similar studies might be useful to further elucidate wood–water interactions in the future as well, though certainly the more complex molecular structure of wood compared to (regular) clay colloids sets limit to modelling possibilities.

Another future application of combined numerical–experimental approaches to wood–water interactions relates to the investigation of hygromechanical couplings, aiming at resolution of the effects of mechanical and moisture loading in a single test setup and extracting all involved material properties therefrom. Such a strategy was adopted for example for clayey soils by Janda et al. (2004), where stiffness and strength parameter as well as the permeability of the soil were derived from a single consolidation test and the temporarily evolving system response.

Hygroexpansion

Moisture uptake also causes dimensional changes, which are a main concern in all outdoor applications of wooden components. Moisture is absorbed when the relative humidity is high and desorbed when in dry conditions. A detailed discussion of the sorption behaviour of wood can be found in Engelund et al. (2012). Wood materials are therefore generally sensitive to changes in climate, and components may warp, buckle or swell/shrink when exposed to climates that are more humid/dry than directly after manufacture. It is often desirable to relate the dimensional instability of wooden structures to that of the constituent materials of the structure. With such understanding, it would be possible to suppress moisture-induced dimensional changes by sensible design of the structure itself or the microstructure of the wood-based material. The complex geometries of components, or the complex microstructure of wooden materials, make it necessary to use numerical models to relate dimensional instability on the structural scale to that on microscale of the materials.

From an engineering point of view, moisture-induced dimensional instability is of special concern in engineered wood-based materials, where the understanding of the link between microstructure and macroscopic swelling can be used in redesign to limit unwanted dimensional swelling. Examples of such materials are wood fibre composites, medium-density fibre boards and kraft liner. These materials are usually supplied as sheets, plates or shells. The layered structure of such materials allows the use of composite mechanics and laminate theory to conceive the linking model. Out-of-plane buckling may arise due to a gradient in moisture content from one side of the material to the other or an asymmetry through the mid-plane in material properties caused by microstructural heterogeneity. Neagu et al. (2005) studied the effect of change in moisture content on out-of-plane buckling in dense wood fibre mats. The macroscopic curvature of the wooden plates was related to the transverse swelling of the constituent entities, that is, the wood fibres. Curvature of large-scale samples is something that is relatively straightforward to measure (see Fig. 7), whereas the average hygroexpansion coefficients of individual wood fibres are

Fig. 7 **a** Measurement of moisture-induced curvature of a thin wooden laminate centrally supported in an upright position, and **b** schematic of curvature induced by a change in relative humidity surrounding a thin wooden sheet (Neagu et al. 2005)

unwieldy to characterize directly. Wood fibres are known to show a very large scatter in properties depending on MFA, wall thickness, polymeric composition, geometry and pit density (e.g. Haygreen and Bowyer 1982). A mixed numerical–experimental method would therefore come in handy to provide an estimate of the fibre hygroexpansion, if the model describes the main swelling mechanisms with sufficient accuracy. The buckling example by Neagu et al. (2005) gives an expression of the macroscopic curvature

$$\kappa = f\left(E_{\mathrm{f}ij}, \beta_{\mathrm{f}ij}, V_{\mathrm{f}}, p(\theta, t)\right)$$

where E_{f} and β_{f} are the elastic and hygroexpansion properties of the fibres, respectively, V_{f} is the volume fraction of fibres, and $p(\theta, t)$ is the fibre orientation distribution through the thickness. Given the structural and elastic properties, the hygroexpansion properties can be identified.

The internal structure of a given solid wood or a wood-based material is relatively complex, and it is usually not sufficient to model the moisture-induced swelling by regarding the material as homogenous and monolithic. Multiscale models are usually required, as exemplified in the example of moisture transport above. The first scale is commonly the macroscopic sample or component, and the next underlying representative scale could be the earlywood and latewood layering, or the wood fibre itself. In the example of warping wooden panels, the link between the two largest scales is provided by classical laminate theory of anisotropic plates. This theory has been widely used in modelling of composite laminates, typically reinforced by carbon or glass fibres. However, the theory was pioneered in the work of Lekhnitskii (1950), where the practical examples were mostly on plywood, which is composed of orthotropic layers, just like carbon or glass fibre composite laminates, published two decades before these were developed. The subsequent underlying link is typically to go from one specific layer to the wood fibre itself, which is a natural representative volume element. This scale can be represented, for example, by a micromechanical model (Marklund and Varna 2009) or a cellular model (Koponen et al. 1991). In this particular example of moisture-induced buckling and thickness expansion (Neagu et al. 2005; Almgren et al. 2010), the transverse hygroexpansion coefficient of the wood fibre can thus be backed out from a simple two-stage model (laminate analogy and micromechanics of a hypothetical unidirectional ply) to be 0.1–0.3 strain per relative humidity, which is roughly in concert with other independent test methods (Wallström et al. 1995; Kajanto and Niskanen 1998).

Mixed numerical–experimental methods may not only prove to be useful in identifying hygroexpansion properties of wood fibres from simple macroscopic tests, otherwise cumbersome to quantify directly. From a general point of view, dimensional instability caused by a change in moisture content is in many respects analogous to thermal deformation of composite materials. The vast literature on thermoelasticy of non-homogenous materials can then inspire modelling efforts in hygroelasticity of wood materials. The main difference between the two cases is that the elastic properties of the wood constituents vary considerably with local moisture content (Cousins 1976, 1978) and that moisture content may depend on the local

hydrostatic pressure (Tremblay et al. 1996). Although these are complicating factors for a straightforward thermoelastic analogy, they are conquerable from a numerical perspective. From an experimental point of view, characterization of dimensional stability necessitates accurate measurements of displacements and the control of the surrounding relative humidity (Badel and Perré 2001). Although the coefficients of thermal expansion of wood is relatively low and results in limited thermal strains within a reasonable temperature range, a moderate change in temperature can affect the equilibrium moisture content which could indirectly lead to non-negligible moisture-induced strains (e.g. Peralta and Skaar 1993). The coupling between temperature, relative humidity, stress state and moisture content is thus a phenomenon that in some cases needs to be considered.

Outlook

The use of mixed numerical–experimental methods is gaining increased use in all areas of materials science, including wood micromechanics. With mixed methods, it is possible to gain understanding and identify material properties, otherwise inaccessible by the separate methods alone. One obstacle is that research practitioners are generally trained within the separate fields of experimental mechanics of numerical modelling. It seems that this obstacle is becoming increasingly surmountable with more integrated education and an increasing number of papers involving an approximately equal amount of matching numerical and experimental work.

Meanwhile, mining from other scientific disciplines in the parameter identification by inverse modelling using mixed numerical–experimental methods can prove to be very useful. Parameter identification is a prolific discipline in itself in control theory, where robust methods to identify governing equations or specific parameters have been developed (e.g. Eykhoff 1974). For instance, an identification method may be ill-posed, that is, the predicted parameter is very sensitive to input data. Regularization of the input data can mitigate some of the problems that arise from the inherent ill-posedness of inverse models (Engl et al. 1996). How the boundary conditions are formulated has shown to have a notable effect on the identification of diffusion parameters in wood materials (Olek et al. 2005). Another challenge is to avoid ending up in a local minimum if optimization procedures are used in parameter identification. The best option seems to be to first systematically vary the initial values in the optimization routines, although it cannot generally be proved that a global minimum has been attained for a black-box model.

Regarding wood micromechanics, mixed methods are likely to be useful in identifying micromechanical properties on a local scale that are not tractable for direct experimental characterization. Some examples have been compiled above in this paper. Specifically, determination of the anisotropic elastic properties of the cell wall by nano-indentation illustrates the synergy between emerging experimental methods and numerical back-calculation. Similar approaches to identify hitherto unknown properties of wood on various length scales are expected in the future. To name a few, phenomena like moisture sorption, hygroexpansion, actuation in living wood, etc. could be addressed in this way.

Conclusion

Some examples of mixed numerical–experimental methods in the micromechanics of wood and fibre-based materials are presented. The irregular microstructure of wood often necessitates a numerical approach to predict the behaviour at larger length scales. The presented examples show how microstructural properties and phenomena can be quantified with a joint approach of experimental measurement and numerical modelling in terms of elasticity, moisture sorption, hygroexpansion and fracture. Future efforts should cope with ill-posedness and numerical sensitivity in the models and direct experimental validation on a local scale. With a balanced and cross-disciplinary approach in modelling and testing, identification of previously undetermined material parameters in the wood microstructure is envisaged.

References

Absetz I (1999) Moisture transport and sorption in wood and plywood: theoretical and experimental analysis originating from wood cellular structure. Helsinki University of Technology, Dissertation

Almgren KM, Gamstedt EK, Varna J (2010) Contribution of wood fibres to the moisture-induced dimensional instability of composite plates. Polym Compos 31:762–771

Avril S, Bonnet M, Bretelle A-S, Grédiac M, Hild F, Ienny P, Latourte F, Lemosse D, Pagano S, Pagnacco E, Pierron F (2008) Overview of identification methods of mechanical parameters based on full-field measurements. Exp Mech 48:381–402

Badel E, Perré P (2001) Using a digital X-ray imaging device to measure the swelling coefficients of a group of wood cells. NDT E Int 34:345–353

Bergander A, Salmén L (2000a) The transverse elastic modulus of the native wood fibre wall. J Pulp Paper Sci 26:234–238

Bergander A, Salmén L (2000b) Variations in transverse fiber wall properties: relations between elastic properties and structure. Holzforschung 54:654–660

Bonfield PW, Ansell MP (1991) Fatigue properties of wood in tension, compression and shear. J Mater Sci 26:4765–4773

Bonnet M, Constantinescu A (2005) Inverse problems in elasticity. IOP Inverse Problems 21:R1–R50

Burgert I, Frühmann K, Keckes J, Fratzl P, Stanzl-Tschegg SE (2003) Microtensile testing of wood fibers combined with video extensometry for efficient strain detection. Holzforschung 57:661–664

Burgert I, Gierlinger N, Zimmermann T (2005) Properties of chemically and mechanically isolated fibers of spruce (*Picea abies* [L.] Karst.). Part 1: structural and chemical characterization. Holzforschung 59:240–246

Cave ID (1969) Longitudinal Young's modulus of pinus radiata. Wood Sci Technol 3:40–48

Cousins WJ (1976) Elastic modulus of lignin as related to moisture content. Wood Sci Technol 10:9–17

Cousins WJ (1978) Young's modulus of hemicellulose as related to moisture content. Wood Sci Technol 12:161–167

Dvinskikh SV, Henriksson M, Berglund LA, Furo I (2011) A multinuclear magnetic resonance imaging (MRI) study of wood with adsorbed water: estimating bound water concentration and local wood density. Holzforschung 65:103–107

Eder M, Jungnikl K, Burgert I (2009) A close-up view of wood structure and properties across a growth ring of Norway spruce (*Picea abies* [L] Karst.). Trees-Struct Funct 23:79–84

Eder M, Arnould A, Dunlop WC, Hornatowska J, Salmén L (2012) Experimental micromechanical characterization of wood cell walls. Wood Sci Technol. doi:10.1007/s00226-012-0515-6

Eitelberger J, Hofstetter K (2010a) Prediction of transport properties of wood below the fiber saturation point—a multiscale homogenization approach and its experimental validation. Part I: thermal conductivity. Compos Sci Technol 71:134–144

Eitelberger J, Hofstetter K (2010b) Prediction of transport properties of wood below the fiber saturation point—a multiscale homogenization approach and its experimental validation. Part II: steady state moisture diffusion coefficient. Compos Sci Technol 71:145–151

Eitelberger J, Hofstetter K (2011) A comprehensive model for transient moisture transport in wood below the fiber saturation point: physical background, implementation and experimental validation. Int J Therm Sci 50:1861–1866

Eitelberger J, Svensson S (2012) The sorption behaviour of wood studied by means of an improved cup method. Transp Porous Med 92:321–335

Eitelberger J, Hofstetter K, Dvinskikh SV (2011a) A multi-scale approach for simulation of transient moisture transport processes in wood below the fiber saturation point. Compos Sci Technol 15:1727–1738

Eitelberger J, Svensson S, Hofstetter K (2011b) Transport processes in wood below the fiber saturation point. Physical background on the microscale and its macroscopic description. Holzforschung 65:337–342

Engelund ET, Thygesen LG, Svensson S, Hill CAS (2012) A discussion on the physics of wood-water interactions. Wood Sci Technol. doi:10.1007/s00226-012-0514-7

Engl HW, Hanke M, Neubauer A (1996) Regularization of Inverse Problems. Kluwer, Dordrecht

Evans R (1999) A variance approach to the X-ray diffractometric estimation of microfibril angle in wood. Appita J 52:283–294

Evans R (2006) Wood Stiffness by X-ray Diffractometry. In: Stokke DD, Groom LH (eds) Characterization of the Cellulosic Cell Wall. Blackwell Publishing, Ames

Eykhoff P (1974) System identification—parameter and system estimation. John Wiley & Sons, New York

Fratzl P, Weinkamer R (2007) Nature's hierarchical materials. Prog Mater Sci 52:1263–1334

Gibson LJ, Easterling KE, Ashby MF (1981) The structure and mechanics of cork. Proc Roy Soc London A 377:99–117

Hameury S, Sterley M (2006) Magnetic resonance imaging of moisture distribution in *Pinus sylvestris* L. exposed to daily indoor relative humidity fluctuations. Wood Mater Sci Eng 1:116–126

Haygreen JG, Bowyer JL (1982) Forest products and wood science. The Iowa State University Press, AMES

Jäger A, Bader T, Hofstetter K, Eberhardsteiner J (2011a) The relation between indentation modulus, microfibril angle, and elastic properties of wood cell walls. Compos Part A 42:677–685

Jäger A, Hofstetter K, Buksnowitz C, Gindl-Altmutter W, Konnerth J (2011b) Identification of stiffness tensor components of wood cell walls by means of nanoindentation. Compos Part A 42:2101–2109

Janda T, Kuklik P, Senjoha M (2004) Mixed experimental and numerical approach to evaluation of material parameters of clayey soils. Int J Geomech 4:199–206

Kajanto I, Niskanen K (1998) Dimensional Stability. Paper Physics. Fapet Oy, Helsinki, In

Keunecke D, Niemz P (2008) Axial stiffness and selected structural properties of yew and spruce microtensile specimens. Wood Res 53:1–14

Keunecke D, Stanzl-Tschegg S, Niemz P (2007) Fracture characterisation of yew (*Taxus baccata* L.) and spruce (*Picea abies* [L.] Karst.) in the radial-tangential and tangential-radial crack propagation system by a micro wedge splitting test. Holzforschung 61:528–388

Keunecke D, Eder M, Burgert I, Niemz P (2008) Micromechanical properties of common yew (Taxus baccata) and Norway spruce (Picea abies) transition wood fibers subjected to longitudinal tension. J Wood Sci 54:420–422

Konnerth J, Buksnowitz C, Gindl W, Hofstetter K, Jäger A (2010) Full set of elastic constants of spruce wood cell walls determined by nanoindentation. In: Proceedings of the International Convention of

the Society of Wood Science and Technology and United Nations Economic Commission for Europe—Timber Committee, Geneva

Koponen S, Toratti T, Kanerva P (1991) Modelling elastic and shrinkage properties of wood based on cell structure. Wood Sci Technol 25:25–32

Krabbenhoft K, Damkilde L (2004) A model for non-Fickian moisture transfer in wood. Mater Struct 37:615–622

Lekhnitskii S (1950) Theory of elasticity of an anisotropic body (in Russian). Gostekhizdat, Moscow

MacMillan MB, Schneider MH, Sharp AR, Balcom BJ (2002) Magnetic resonance imaging of water concentration in low moisture content wood. Wood Fiber Sci 34:276–286

Marklund E, Varna J (2009) Modeling the hygroexpansion of aligned wood fiber composites. Compos Sci Technol 69:1108–1114

Morais J, Xavier J, Pereira J, Pinto L (2011) Book of abstracts of the COST Action FP0802 Thematic workshop: Mixed numerical and experimental methods applied to the mechanical characterization of bio-based materials, University of Trás-os-Montes e Alto Douro, Vila Real, April 27–28. Vila Real, Portugal

Mott L, Groom L, Shaler S (2002) Mechanical properties of individual Southern Pine fibers. Part II. Comparison of earlywood and latewood fibers with respect to tree height and juvenility. Wood Fib Sci 34(2):221–237

Neagu RC, Gamstedt EK, Lindström M (2005) Influence of wood-fibre hygroexpansion on the dimensional instability of fibre mats and composites. Compos Part A 36:772–788

Neagu RC, Gamstedt EK, Bardage SL, Lindström M (2006) Ultrastructural features affecting mechanical properties of wood fibres. Wood Mater Sci Eng 1:146–170

Nguyen TQ, Petkovic J, Dangla P, Baroghel-Bouny V (2008) Modelling of coupled ion and moisture transport in porous building materials. Construct Build Mater 22:2185–2195

Olek W, Perré P, Weres J (2005) Inverse analysis of the transient bound water diffusion in wood. Holzforschung 59(1):38–45

Olek W, Perré P, Weres J (2011) Implementation of a relaxation equilibrium term in the convective boundary condition for a better representation of the transient bound water diffusion in wood. Wood Sci Technol 45(4):677–691

Oliver WC, Pharr GM (1992) Improved technique for determining hardness and elastic modulus using load and displacement sensing indentation experiments. J Mater Res 7:1564–1580

Orso S, Wegst UGK, Arzt E (2006) The elastic modulus of spruce wood cell wall material measured by an in situ bending technique. J Mater Sci 41:5122–5126

Östlund S, Nilsson F (1993) Cohesive modelling of damage at the tip of cracks in slender beam structures. Fatigue Fract Eng Mater Struct 16:663–676

Pel L, Brocken H, Kopinga K (1996) Determination of moisture diffusivity in porous media using moisture concentration profiles. Int J Heat Mass Transfer 39:1273–1280

Peralta PN, Skaar C (1993) Experiments on steady-state non-isothermal moisture movement in wood. Wood Fib Sci 25:124–135

Perré P (2007) Multiscale aspects of heat and mass transfer during drying. Transp Porous Media 66:59–76

Pharr GM, Oliver WC, Brotzen FR (1992) On the generality of the relationship among contact stiffness, contact area, and elastic modulus during indentation. J Mater Res 7:613–617

Porion P, Delville A (2009) Multinuclear NMR study of the structure and micro-dynamics of counterions and water molecules within clay colloids. Curr Opin Colloid Interface Sci 14:216–222

Quick JJ, Hailey JRT, Mackay AL (1990) Radial moisture profiles of cedar sapwood during drying—a proton magnetic-resonance study. Wood Fiber Sci 22:404–412

Reiterer A, Lichtenegger H, Tschegg S, Fratzl P (1999) Experimental evidence for a mechanical function of the cellulose microfibril angle in wood cell walls. Philo Mag A—Phys Condens Matter Struct Defects Mech Prop 79:2173–2184

Rikards R (2003) Identification of mechanical properties of laminates. In: Altenbach H, Becker W (eds) Modern trends in composite laminates mechanics. Springer, Wien, pp 181–225

Schirmer R (1938) Die Diffusionszahl von Wasserdampf-Luft-Gemischen und die Verdampfungsgeschwindigkeit, Ph.D. thesis, Technische Hochschule München

Schreier HW, Garcia D, Sutton MA (2004) Advances in light microscope stereo vision. Exp Mech 44:278–287

Shipsha A, Berglund LA (2007) Shear coupling effects on stress and strain distributions in wood subjected to transverse compression. Compos Sci Technol 67:1362–1369

Siau JF (1984) Transport processes in wood. Verlag Springer, Berlin

Sol H, Oomens CWJ (1997) Material identification using mixed numerical experimental methods. Kluwer, Dordrecht

Sørensen BF, Jacobsen TK (1998) Large-scale bridging in composites: R-curves and bridging laws Compos Part A 29:1443–1451

Sørensen BF, Jacobsen TK (2003) Determination of cohesive laws by the J integral approach. Eng Fract Mech 70:1841–1858

Sørensen BF, Gamstedt EK, Østergaard RC, Goutianos S (2008) Micromechanical model of cross-over fiber bridging—Prediction of mixed mode bridging law. Mech Mater 40:220–234

Spearing SM, Evans AG (1992) The role of fiber bridging in the delamination resistance of fiber-reinforced composites. Acta Metal Mater 40:2191–2199

Sutton MA, Ke X, Lessner SM, Goldbach M, Yost M, Zhao F, Schreier HW (2008) Strain field measurements on mouse carotid arteries using microscopic three-dimensional digital image correlation. J Biomed Mater Res 84A:178–190

Swadener JG, Pharr GM (2001) Indentation of elastically anisotropic half-spaces by cones and parabolae of revolution. Phil Mag A 81:447–466

Tarantola A (2005) Inverse problem theory and methods for model parameter estimation. SIAM, Philadelphia

Tremblay C, Cloutier A, Fortin Y (1996) Moisture content-water potential relationship of red pine sapwood above the fiber saturation point and determination of the effective pore size distribution. Wood Sci Technol 30:361–371

Vantomme, J, De Visscher J, Sol H, De Wilde WP (1995) Determination and parametric study of material damping in fibre reinforced plastics: a review. Eur J Mech Eng 40: No 4

Vlassak JJ, Ciavarella M, Barber JR, Wang X (2003) The indentation modulus of elastically anisotropic materials for indenters of arbitrary shape. J Mech Phys Solids 51:1701–1721

Wallström L, Lindberg KAH, Johansson J (1995) Wood surface stabilization. Holz Roh Werkst 53:87–92

Wang G, Yu Y, Shi SQ, Wang JW, Cao SP, Cheng HT (2011) Microtension test method for measuring tensile properties of individual cellulosic fibers. Wood Fib Sci 43(3):251–261

Waszczyszyn Z, Burczynński T, Mróz Z (2009) Special issue: papers from the international symposium on inverse problems in mechanics of structures and materials—IPM 2009. Inv Prob Sci Eng 19:1–153

Yoshihara H, Tsunematsu S (2007) Bending and shear properties of compressed Sitka spruce. Wood Sci Technol 45:117–131